

TITLE: EFFECTS OF TURBULENCE ON LOW ALTITUDE FIREBALLS AT LATE TIMES

AUTHOR(S): H. M. Ruppel and R. A. Gentry

SUBMITTED TO: PROCEEDINGS OF DNA ATMOSPHERIC EFFECTS SYMPOSIUM

By acceptance of this article for publication, the publisher recognizes the Government's (license) rights in any copyright and the Government and its authorized representatives have unrestricted right to reproduce in whole or in part said article under any copyright secured by the publisher.

The Los Alamos Scientific Laboratory requests that the publisher identify this article as work performed under the auspices of the U. S. Atomic Energy Commission.



los alamos
scientific laboratory
 of the University of California
 LOS ALAMOS, NEW MEXICO 87544

NOTICE

This report was prepared as an account of work sponsored by the United States Government. Neither the United States nor the United States Atomic Energy Commission, nor any of their employees nor any of their contractors, subcontractors, or their employees, makes any warranty, express or implied, or assumes any legal liability or responsibility for the accuracy, completeness or usefulness of any information, apparatus, product or process disclosed, or represents that its use would not infringe privately owned rights.

MASTER

UNLIMITED

EFFECTS OF TURBULENCE ON
LOW ALTITUDE FIREBALLS AT LATE TIMES* (U)

H. M. Ruppel and R. A. Gentry
Los Alamos Scientific Laboratory
University of California
Los Alamos, New Mexico 87544

Let us precede a discussion of the effects of turbulence on the dynamics of fireballs with a review of the turbulence model currently in use at Los Alamos.¹ The equations we solve are:

the mass equation

$$\frac{\partial \rho}{\partial t} + \frac{\partial}{\partial x_j} \rho u_j = \frac{\partial}{\partial x_j} \sigma \frac{\partial \rho}{\partial x_j} ,$$

the momentum equation

$$\begin{aligned} \frac{\partial}{\partial t} \rho u_j - \frac{\partial}{\partial t} \sigma \frac{\partial \rho}{\partial x_j} + \frac{\partial}{\partial x_1} \rho u_1 u_j = & s_j \\ & + \frac{\partial}{\partial x_1} \left(p_{1j} + \rho \sigma a_{1j} - \frac{2}{3} \rho \left(q + \frac{1}{2} \sigma a_{l,k} \right) \delta_{1j} + \sigma \left(u_1 \frac{\partial \rho}{\partial x_j} + u_j \frac{\partial \rho}{\partial x_1} \right) \right) . \end{aligned}$$

the internal energy equation

$$\frac{\partial \rho I}{\partial t} + \frac{\partial \rho u_j I}{\partial x_j} = p_{1j} \frac{\partial u_1}{\partial x_j} + \frac{100 \rho \sigma q}{a^2} + \frac{\partial}{\partial x_j} \sigma \frac{\partial \rho I}{\partial x_j} ,$$

*This work was performed under the joint auspices of the United States Atomic Energy Commission and the Defense Nuclear Agency (DNA Subtask No. HC-061, DNA Work Unit No. 15--Calculations at Low Altitude).

and the turbulence energy equation

$$\frac{\partial \rho q}{\partial t} + \frac{\partial}{\partial x_j} \rho u_j q = - \frac{\sigma}{\rho} \frac{\partial \rho}{\partial x_j} \frac{\partial p}{\partial x_j} + \rho \sigma e_{ij} \frac{\partial u_j}{\partial x_i} - \frac{1}{3} \rho e_{kk} \left(q + \frac{1}{2} \sigma e_{kk} \right) - \frac{100 \rho \sigma q}{2} + \frac{\partial}{\partial x_j} \sigma \frac{\partial \rho q}{\partial x_j} .$$

In the above

$$\sigma = 0.02s \sqrt{2q}$$

$$e_{ij} = \frac{\partial u_i}{\partial x_j} + \frac{\partial u_j}{\partial x_i} .$$

and

$$p_{ij} = - p \delta_{ij} + \frac{1}{2} \lambda e_{kk} \delta_{ij} + \mu e_{ij} .$$

A detailed list of the symbols used is included as Appendix A.

The salient feature of this and several other similar models now in use is the transport equation for the turbulence energy. This equation contains creation due to buoyancy and shear, and dissipation and diffusion. Consider in particular the buoyancy term, since this has engendered some comment in the recent past. In this connection note that one models correlations between components of velocity and other scalar functions as

$$\overline{u_i f} = - \sigma \frac{\partial f}{\partial x_i} .$$

This is commonly referred to as the flux approximation. Using this approximation in reverse for $- \sigma \frac{\partial \rho}{\partial x_j}$ leads to

$$- \frac{\sigma}{\rho} \frac{\partial \rho}{\partial x_j} \frac{\partial p}{\partial x_j} = \frac{1}{\rho} \frac{\partial p}{\partial x_j} \overline{\rho u_j} .$$

Then assuming hydrostatic equilibrium we obtain

$$-\frac{\sigma}{\rho} \frac{\partial p}{\partial x_j} \frac{\partial \rho}{\partial x_j} = g \overline{\rho' u'}$$

Hence a nice physical interpretation of this term is to view it as the contribution to the change in turbulence energy from changes in the potential energy due to the correlation of fluctuations of density and velocity in a gravitational field. Note that in order to have creation rather than destruction of turbulence energy, the density and pressure gradients must be of opposite sign.

An assumption which is made in the derivation of this model is that there exists immediately a state of equilibrium between eddies of all sizes. We assume, in other words, that the time taken to equilibrate the cascade process by which energy is transferred from the largest eddies where it is created to the smallest eddies where it is dissipated is small compared to the times that matter in the problem. Current estimates for this equilibration time in fireballs vary from perhaps one tenth to one torus formation time, but these numbers are uncertain.

Another assumption which must be made in calculations with this model is the size of the integral scale - that is the size of the largest or energy carrying eddies. What we use for the scale is a phenomenological form fitted by Bart Daly at Los Alamos to the experiments of Wagnanski and Fiedler.² They measured the scale and the mean vertical velocity profiles of free jets. It was possible to fit their data rather well with the form

$$s(r, z) = 0.14 d(z) \left(2 - \frac{v(r, z)}{v(0, z)} \right)$$

In this expression $d(z)$ is taken to be that distance at a given z from the axis to the point at which the vertical component of velocity changes sign. In some approximation, then, in the region of interest $d(z)$ is the radius to the point of maximum amplitude of vorticity. Also $v(0, z)$ is the vertical velocity on the axis at a given z ; $v(r, z)$ is the vertical velocity at r and z . This form gives a scale which has its minimum on the axis and rises to a maximum where $v(r, z)$ vanishes. When $v(r, z)$ becomes negative, we simply set it to zero. This, then, leads to a scale which varies from perhaps 1/20th to 1/5th km over the fireball. Figures 1 and 2 give an indication of the effect of the scale on the turbulence energy. Figure 1 is a plot of the maximum in any cell and Fig. 2 a plot of the total turbulence energy, each for two different scales. In both cases the dashed curve was calculated with a scale, $s = 0.1$, constant over the mesh while the solid curve was obtained with a simplified version of the phenomenological scale discussed above. The scales differ by about a factor of 3 and the energies by roughly an order of magnitude. One can argue credibly that this is a consistent picture by equating the creation and decay at steady state. Since the creation is proportional to $\sigma \times$ mean flow quantities and the decay is proportional to $\sigma q/s^2$, one has

$$\sigma A = \sigma B q / s^2 ,$$

where A and B are combinations of constants and mean flow quantities. If then the mean flow is roughly independent of the scale, this results in

$$q \sim s^2 .$$

This argument is to be taken only as an indication of the order of the effect of the scale on the turbulence energy. In the example of the large scale case the total turbulence energy remains at about 1% of the total kinetic energy in the mesh.

For the value of σ that we use it is interesting to note that the rise altitude, as defined by the position of the cell with the maximum internal energy, is little affected by changes in the scale. Figure 3 displays the altitude as a function of time for two scales. The \times 's were obtained with a scale larger than the solid curve, the increase being 50%; however, at 210 secs there is only a 1/2 km difference in height. There appears to be no difference in the two calculations for times less than 75 secs. This last point has been a consistent finding in our calculations - that the turbulence has virtually no effect on dimensional data at less than 75 secs and only a slight effect thereafter. This conclusion may depend on the rather small value for σ that we are using.

Although there is general agreement of models of this type that σ may be expressed as $\sigma = \beta s \sqrt{2q}$, the values of β differ among the various investigators. We currently use a value of $\beta = 0.02$ which value is based on the work of Laufer, Morse, Rodi, and Spalding.³ They compared six turbulence models in the prediction of free shear flows. In the model which they call the Prandtl energy model they define a turbulence viscosity which is analogous to the above σ and in comparison with experiment they arrive at the value for β which we are currently using. Daly then performed an independent check by testing this result against the channel flow studies of Laufer,⁴ who measured both the Reynolds stress and the gradient of the mean velocity. Using the flux approximation one can relate the two to obtain σ . This was done for Reynolds numbers in the range 10^4 to 10^8 .

Another point which must be addressed is the seeding of the initial turbulence. From the equation for the turbulence energy it is clear that in order to generate turbulence it is necessary that some turbulence be already present. In the real fireball, instabilities serve to initiate the turbulence. In our numerical simulations we must seed the turbulence in some way.

Figure 4 demonstrates the independence of the late time turbulence level and distribution on the method and level of seeding. It displays contour plots of the turbulence energy for two rather different seedings. In the upper plots the turbulence was seeded as proportional to the vorticity while in the lower plots as proportional to the kinetic energy. Clearly the two

methods of seeding yield marked differences in level and configuration initially, but by 30 secs they have coalesced into a single distribution. What has happened is that the turbulence has decayed away in regions which cannot support it and has grown in those places where shear and buoyancy can support it.

Figure 5 indicates how rather local the shear creation, in fact, is; the same is true of the buoyancy creation. Moreover, the region of largest shear creation is at the upper edge of the fireball, and hence turbulence is most pronounced in the region of steepest temperature gradients. One might expect that the turbulence will reduce the maximum gradients and that is indeed what we find. In Fig. 6 there is a comparison of the maximum gradient of internal energy calculated with and without turbulence. Both of these were carried out with a fine grid and indicate what is probably the major effect we will find that turbulence has: the degrading of temperature and density gradients.

Of course the turbulence itself depends crucially on the gradients of the mean flow; both the shear and the buoyancy creation are products of mean flow gradients. It is this which causes us to devote such effort to improve our non-turbulent calculations, particularly as they affect temperature and density gradients. If these are overly diffused by numerical effects, little is gained by simply adding turbulence to the hydrodynamics. To achieve this we use an ALE-like code⁵ which allows the cells to follow the fluid motion as much as is possible. This minimizes the amount of fluxing in the rezone process and reduces the diffusion of all the physical quantities and their gradients.

One can see the effect of resolution on turbulence energy by comparing contour plots from a high resolution calculation with a low resolution result at 20 secs as in Fig. 7. The fine grid calculation has a maximum turbulence energy of 1.2×10^{-4} while the coarse grid on the right has a maximum of 8.5×10^{-5} . The total turbulence energy differs by about the same ratio. Since the minimum cell size in the two calculations differs by a factor of 2-1/2 and the turbulence energy by only 50%, it is reasonable to assume that further refining of the zone size will not greatly affect the amount of turbulence energy. Note also that the configuration of the two calculations in Fig. 7 are similar in appearance.

As a reference, note that the maximum vertical velocity is about 0.14 km/sec. The maximum turbulence energy corresponds to a fluctuating velocity of 0.01 km/sec or roughly 10% of the maximum mean flow velocity. Finally let us return to the effect of turbulence on dimensional data.

Figure 8 displays a rise history for a coarse grid calculation with and without turbulence. The inclusion of the added viscosity due to turbulence causes only a slight decrease in altitude at late times. It is, however,

conceivable that as better calculations with sharper gradients are performed, higher levels of turbulence may be supported which increase the net effect. In addition a larger value of β would likely lead to more pronounced differences due to turbulence.

REFERENCES

1. B. J. Daly and F. H. Harlow, *Phys. Fluids* 13, 2634 (1970).
2. I. Wagnanski and H. Fiedler, *J. Fluid Mech.* 38, 577 (1969).
3. B. E. Launder et al., Imperial College Report TM/TN/B/19.
4. J. Laufer, NACA Report No. 1053 (1951).
5. A. A. Amsden and C. W. Hirt, "YAQUI: An Arbitrary Lagrangian-Eulerian Computer Program for Fluid Flows at All Speeds," Los Alamos Scientific Laboratory report LA-5100.

APPENDIX A

Notation

- ρ = density
- t = time
- x_j = j^{th} coordinate
- u_j = j^{th} component of velocity
- σ = turbulence viscosity
- s = integral scale
- q = specific turbulence energy
- g_j = gravitational acceleration in j th direction
- p = pressure
- λ = dilational viscosity
- μ = shear viscosity
- δ_{ij} = Kronecker delta function
- I = specific internal energy

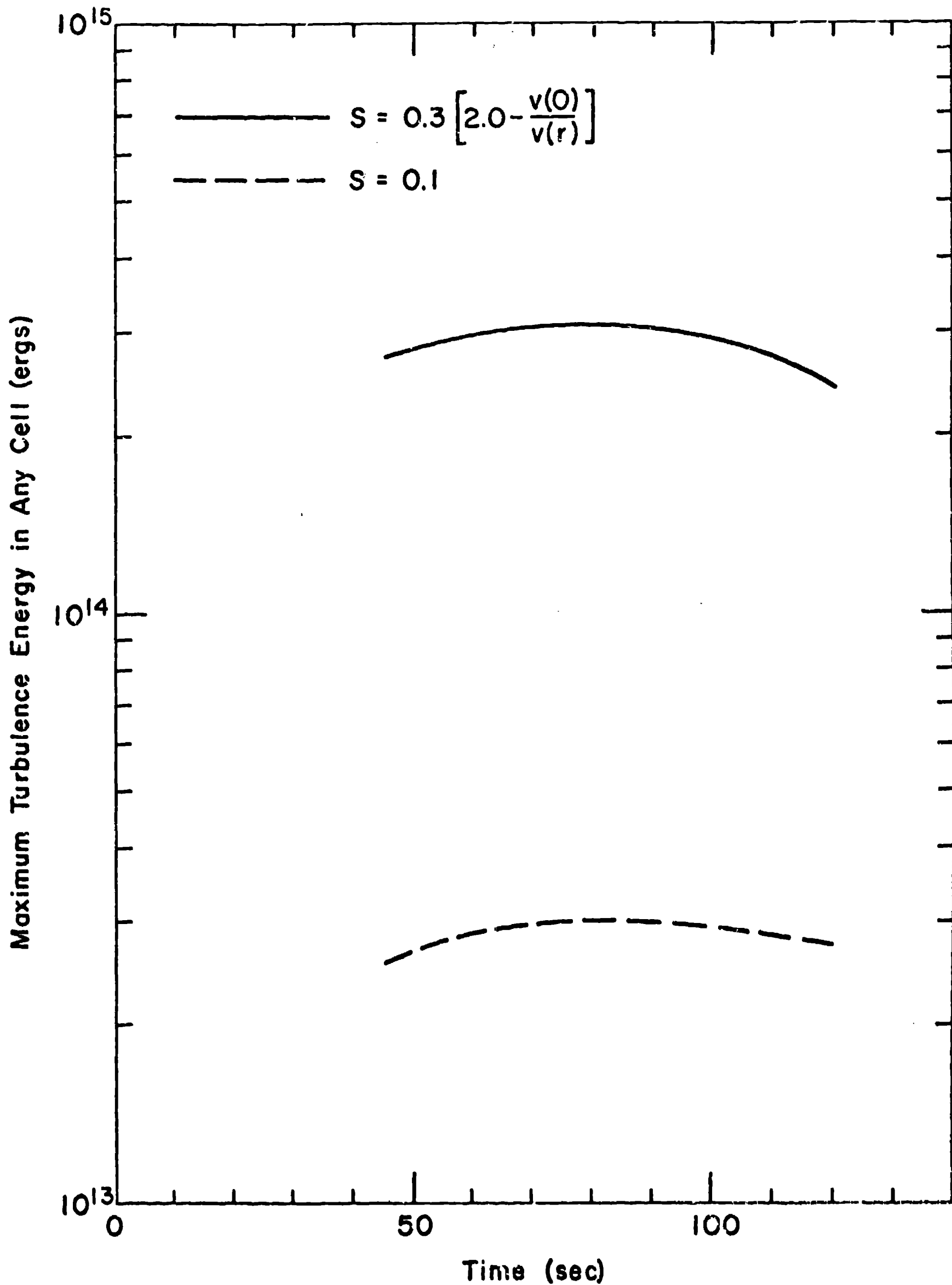


Fig. 1. Maximum turbulence energy in any computational cell for two integral scales.

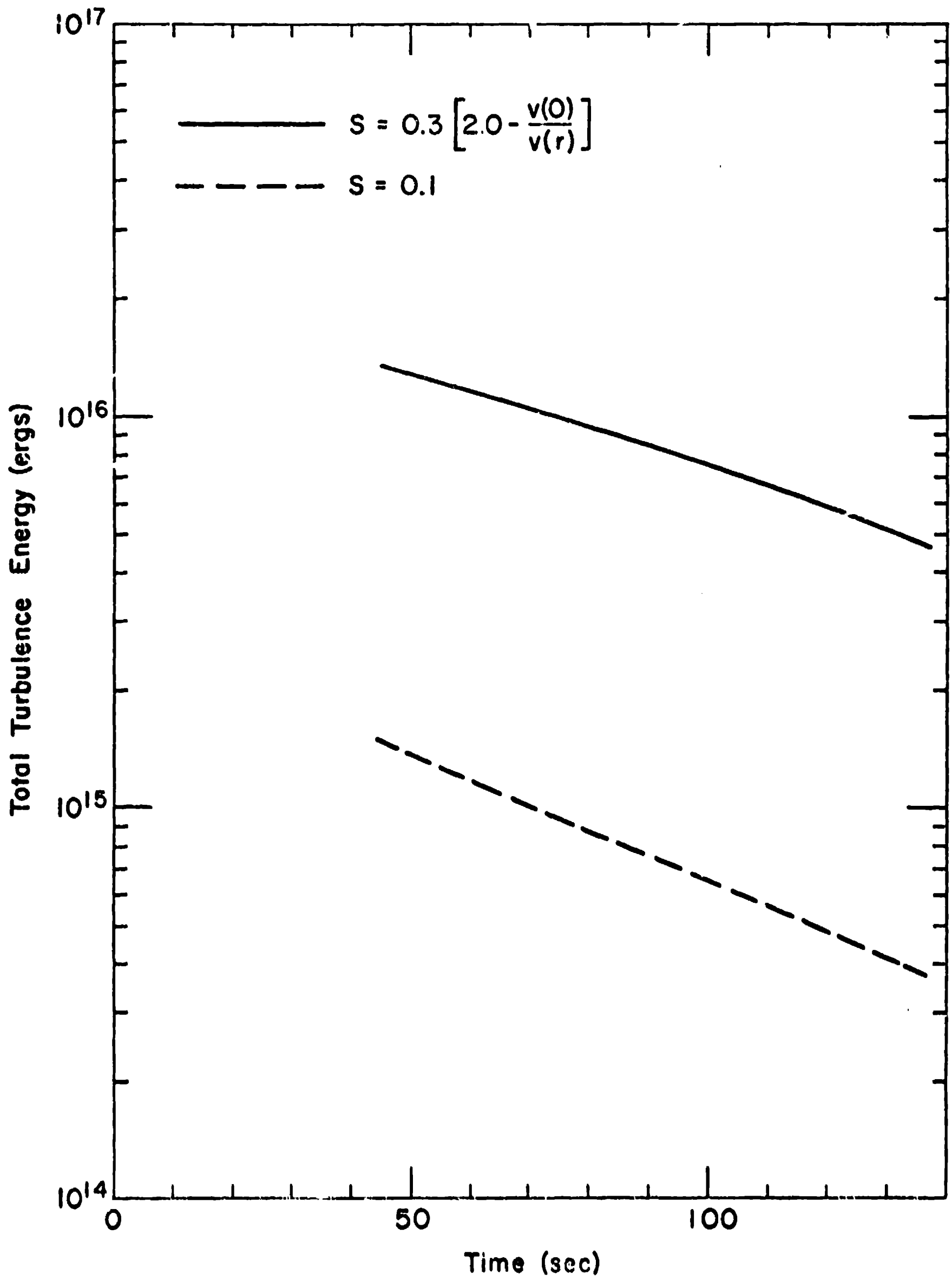


Fig. 2. Total turbulence energy in the mesh for two integral scales.

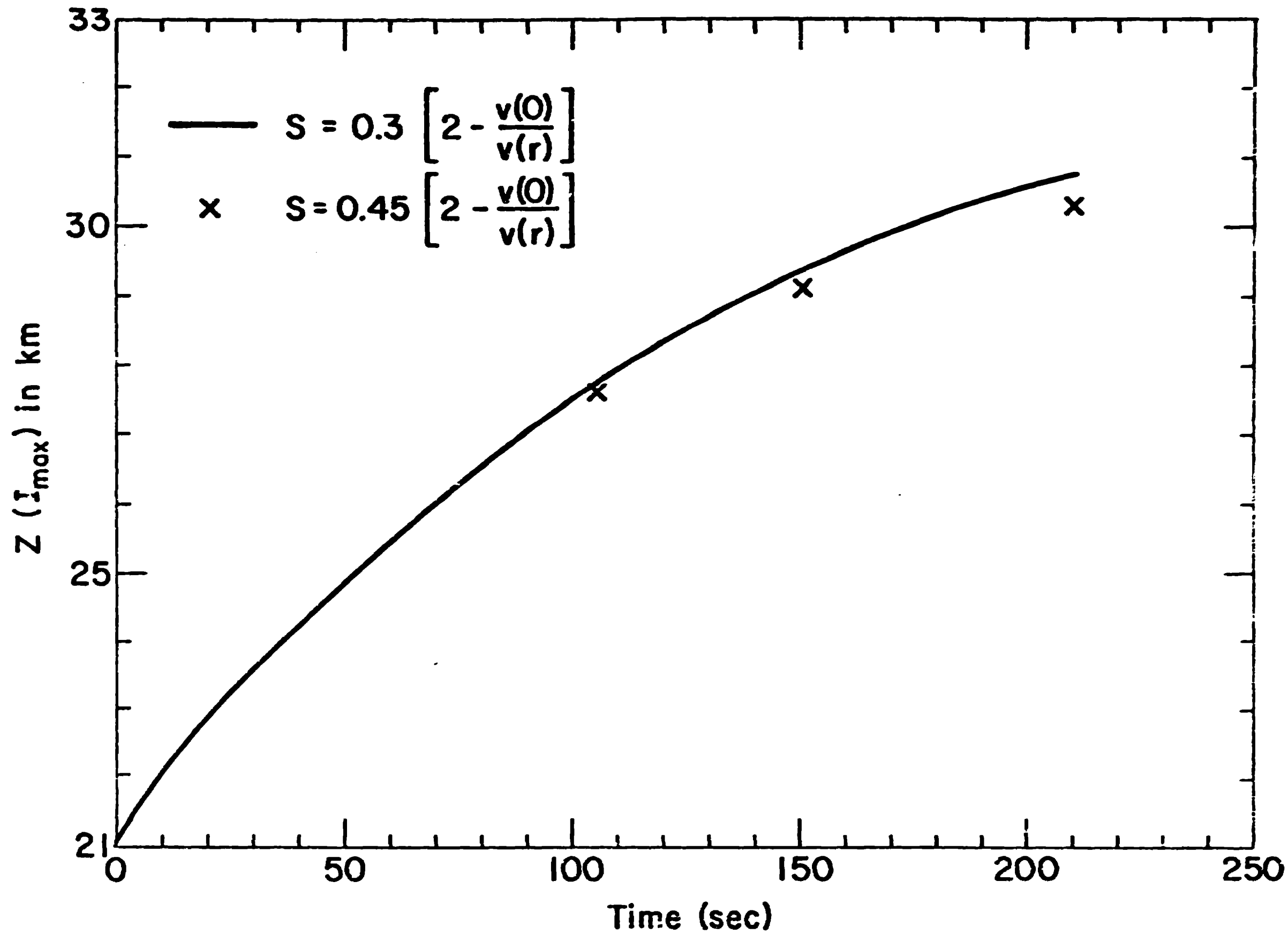
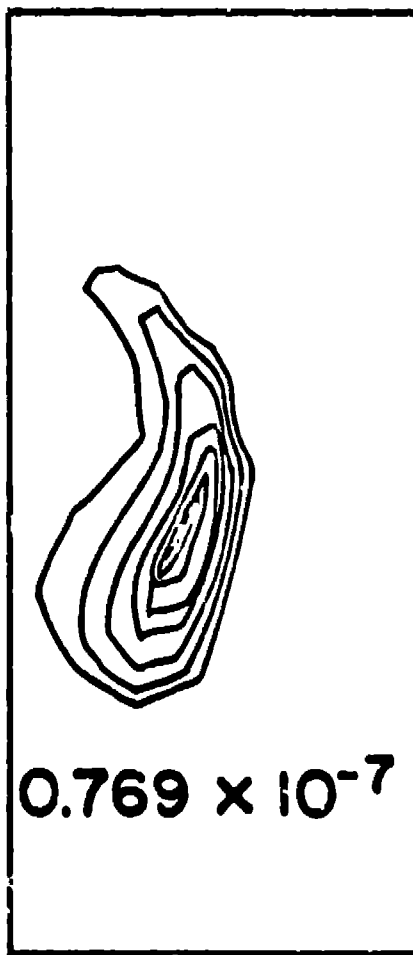


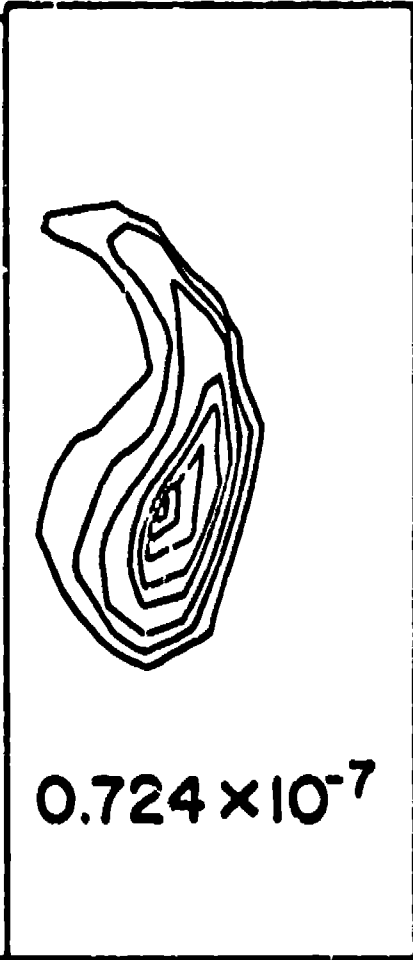
Fig. 3. Altitude as a function of time for two scales, one 50% larger than the other.

Turbulence Energy

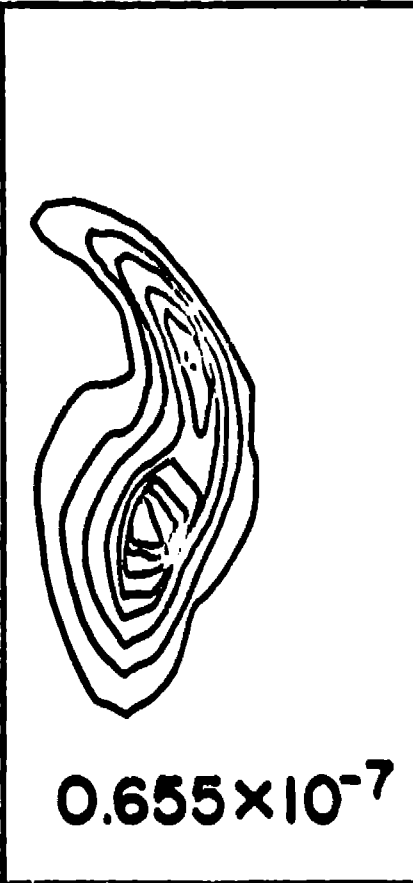
$q \sim \epsilon$



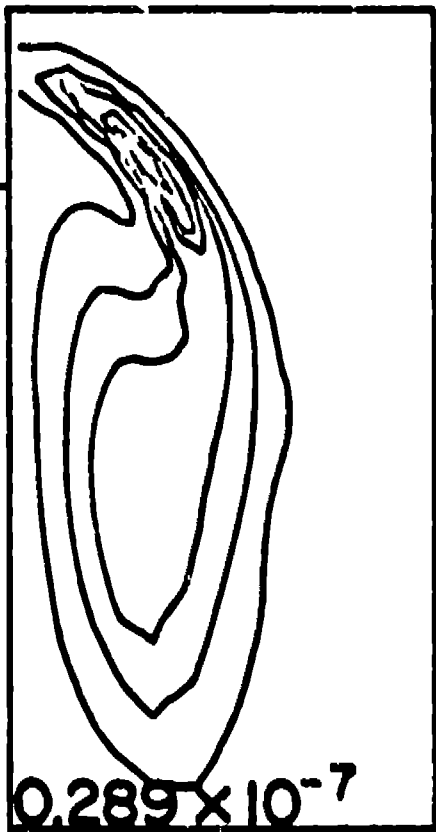
$t = 7.35$



$t = 8$



$t = 10$



$t = 30$

$q \sim KE$

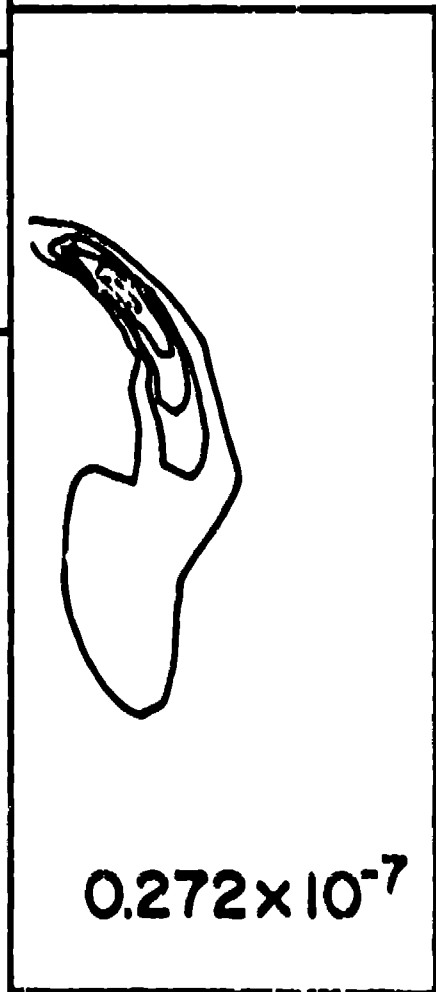
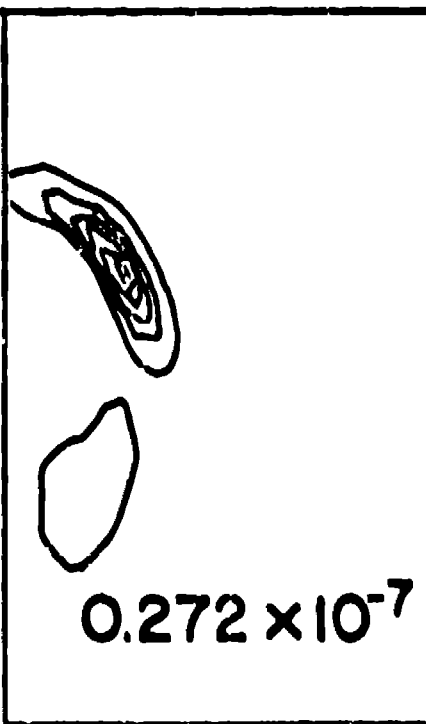
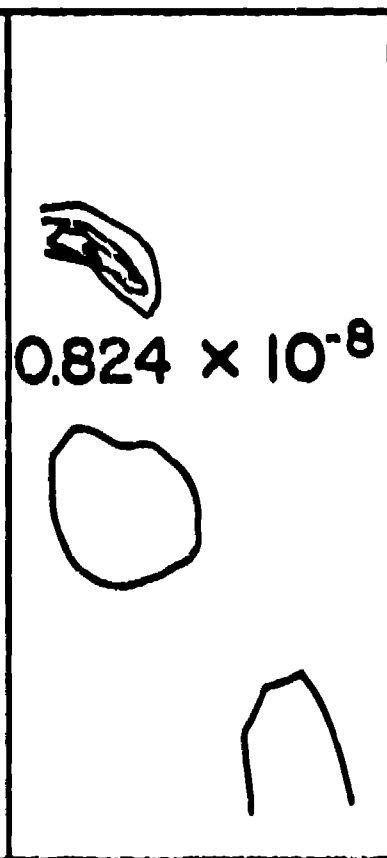
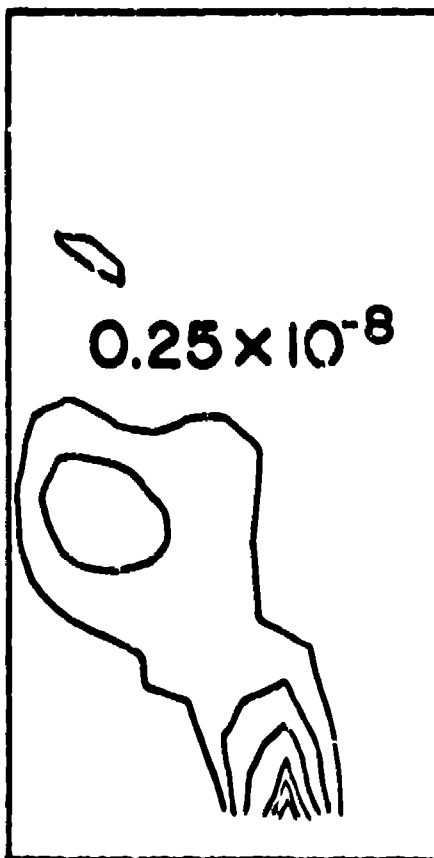


Fig. 4. Turbulence energy contours for four times with two different initial distributions.

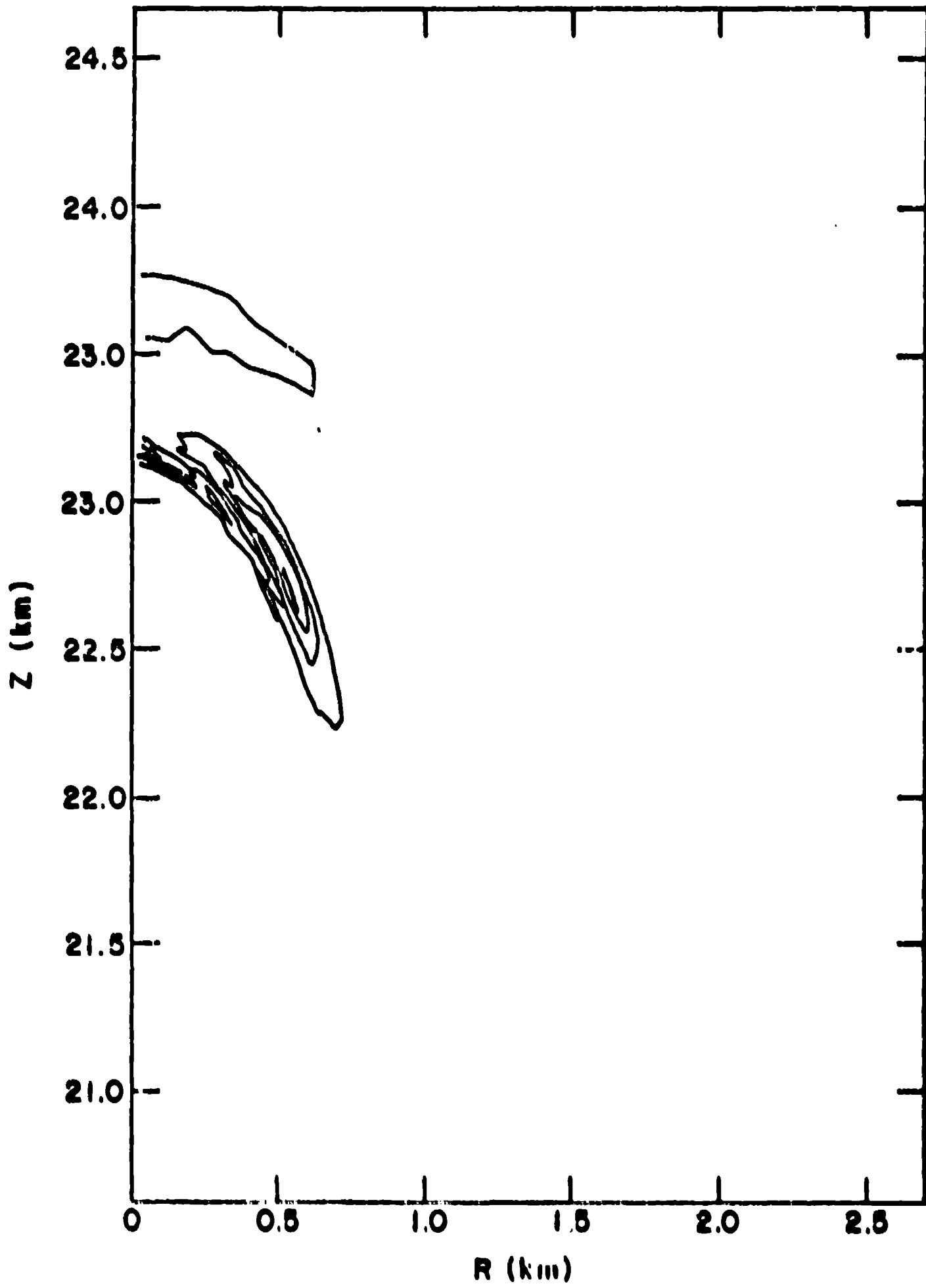


Fig. 5. Contour plot of shear creation.

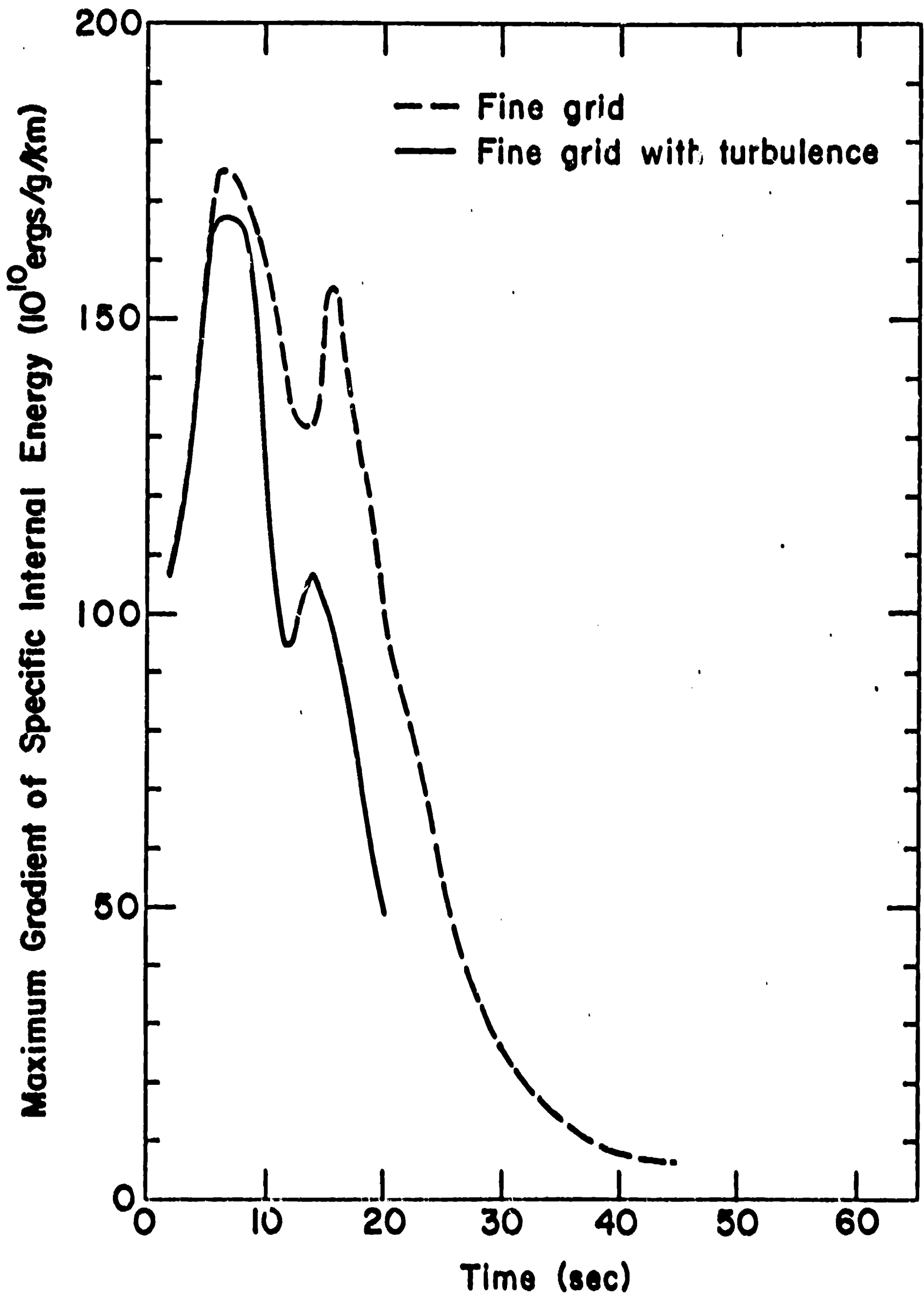


Fig. 6. Maximum gradient of internal energy with and without the inclusion of turbulence.

$t = 20 \text{ sec}$

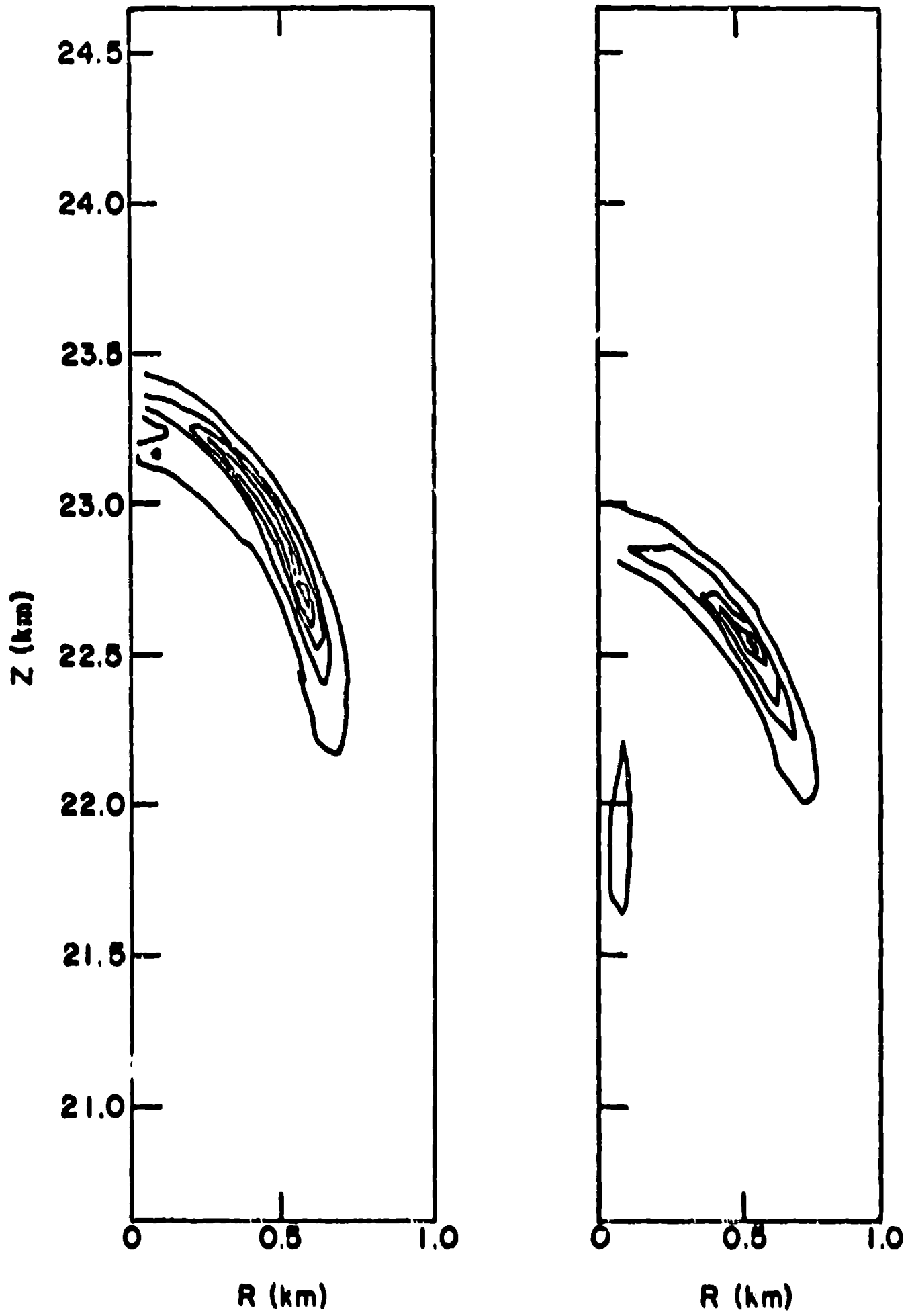


Fig. 7. Contour plots of turbulence energy for fine grid (left) and coarse grid (right) calculations.

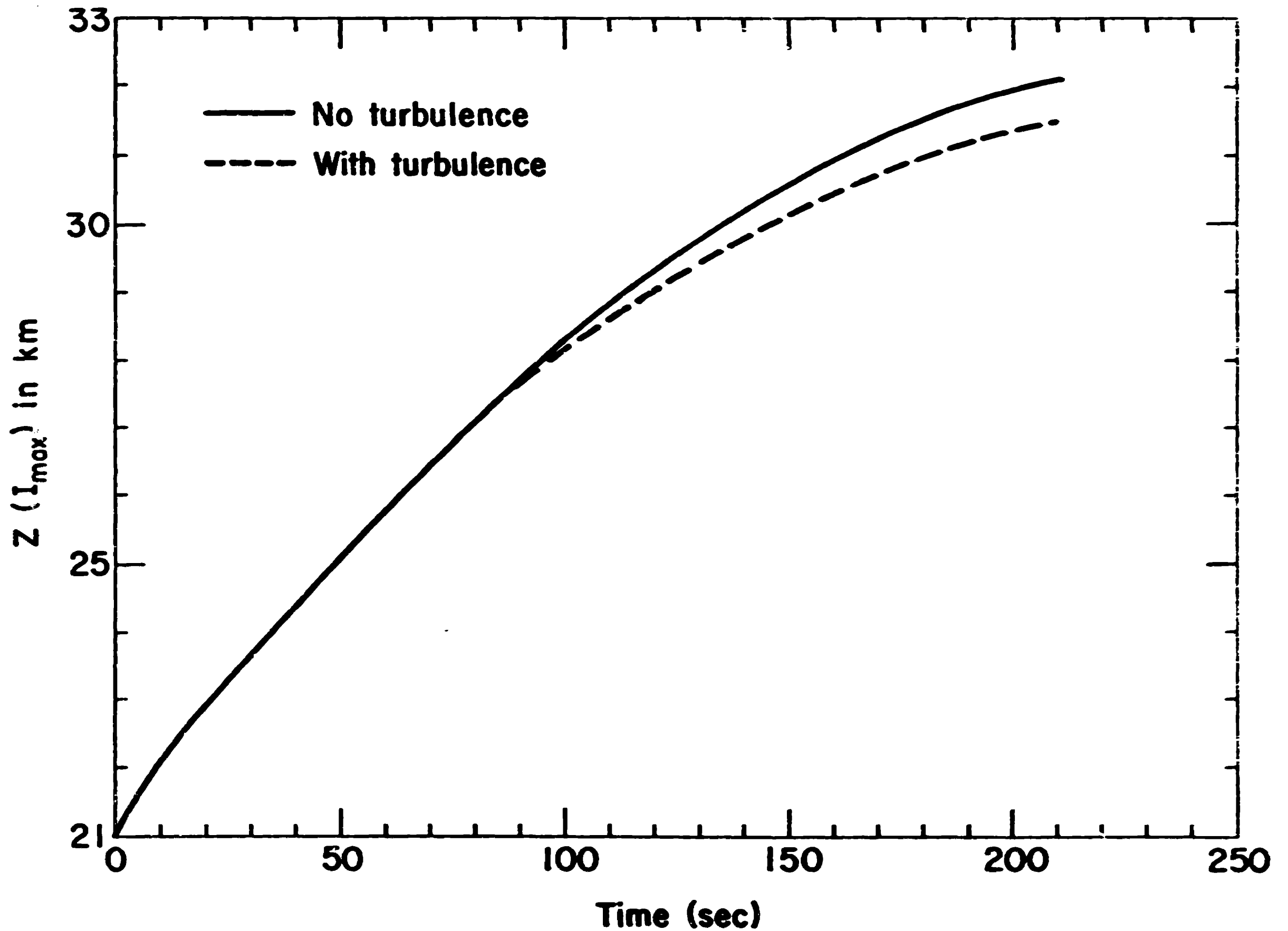


Fig. 8. Altitude as a function of time for a coarse grid calculation, with and without the inclusion of turbulence.